

INSTITUTE OF PAPER SCIENCE AND TECHNOLOGY

Atlanta, Georgia

FUNDAMENTALS OF ACOUSTIC RADIATION PRESSURE

Project F008

Report 2

Covered Period: July 1994–December 1994

A Progress Report

to the

MEMBER COMPANIES OF THE INSTITUTE OF PAPER SCIENCE AND TECHNOLOGY

By

P.H. Brodeur

February 1995

TABLE OF CONTENTS

OBJECTIVES.....3

SUMMARY3

VALUE TO THE INDUSTRY.....4

PROJECT HISTORY6

ACCOMPLISHMENTS.....6

EXPERIMENTAL SETUP8

ACOUSTIC WET FIBER FLEXIBILITY13

ACOUSTIC COMPACTIBILITY OF A FIBER MAT15

ACOUSTIC FIBER SEPARATION/FRACTIONATION17

ACOUSTIC FIBER AGGLOMERATION AND REORIENTATION.....19

A. OPTICAL MONITORING SYSTEMS.....19

B. CURRENT EXPERIMENTS.....20

B.1 Speed of Fiber Agglomeration.....21

B.2 Rotation of Fibers During Agglomeration.....21

LITERATURE CITED.....22

OBJECTIVES

- Investigate fundamentals of acoustic radiation pressure (ARP) effects on fiber suspensions;
- Investigate mechanisms of acoustic fiber agglomeration and reorientation;
- Demonstrate the concept of acoustic wet fiber flexibility/compactibility;
- Demonstrate the concept of acoustic fiber separation/fractionation;
- Explore other process-related applications of acoustic radiation pressure, acoustic cavitation, and acoustic streaming;
- Determine the economic viability of acoustically-based industrial processes.

SUMMARY

The development of an experimental research program to study various effects of acoustic radiation pressure on water suspended fibers was continued. The program was sufficiently mature to be structured into several interrelated subprojects: acoustic cell characterization, acoustic wet fiber flexibility, acoustic compactibility of a fiber mat, acoustic fiber separation/fractionation, and acoustic fiber reorientation.

Regarding the characterization of the acoustic cell, a relationship was obtained between the electrical power delivered to the transducer and the acoustic power. Also, two independent methods were tested to determine the acoustic radiation force. Results were used to validate the procedure to measure the acoustic power.

In the area of wet fiber flexibility, observations of cantilever-mounted fibers subjected to a distributed acoustic load indicated that the fibers did not bend as expected. Instead, some fibers

could not sustain the acoustic load and were sectioned. This “refining” effect was attributed to an apparent increase of fiber stiffness due to the 150 kHz oscillating load. This is a consequence of the viscoelasticity of wood pulp fibers.

Unexpected results about fiber flexibility triggered the development of a modified setup to investigate the compactibility of a wet fiber mat due to a traveling wave field. A series of preliminary experiments were performed using softwood fibers beaten to various levels using a Valley beater. Results were obtained at 0.5% and 1% consistency. A relationship was found between the beating time and the differential cross-sectional area of the fiber mat as obtained with and without the acoustic load. Measurements did not appear to be sensitive to consistency.

We decided to go ahead with the development of a prototype acoustic fiber separation/fractionation system. A traveling wave field separation configuration was implemented. An adjustable mechanical divider with two output streams was installed above the acoustic cell to collect coarser and slender fibers. Preliminary trials using softwood fibers at 0.5% consistency indicated that the system was capable of producing high and low consistency fractions.

Finally, the laser-based optical monitoring system to study acoustic fiber agglomeration and reorientation was fully implemented.

VALUE TO THE INDUSTRY

The long-term streamline of project F008 is to provide the scientific and technical basis for the development of novel ultrasonic instruments and/or processing technologies that would benefit the pulp and paper industry.

Possible outcomes of the current work about acoustic fiber flexibility/compactibility would be the development of on-line instrumentation for fiber compactibility and refining monitoring and the development of acoustic refining technologies.

Research about the use of an acoustic field to separate and/or fractionate wood pulp fibers might lead to the development of on-line adaptable industrial fiber separation processes. As acoustic fractionators might be capable of processing continuously varying furnishes or be reprogrammed to meet different separation requirements, they could considerably increase the return on capital investment. As an example, while pressure-screen fractionators are dedicated mechanical systems, acoustically-based fractionators, which would be free of moving parts, might provide far more flexibility by allowing electrically-driven parameters to control separation.

Acoustic forming, which would be an evolved concept of acoustic separation, might provide the basis for furnish/product adaptable forming processes and diversify the use of a paper machine. Here again, the return on capital investment might be very high. One can envision among other concepts acoustic positioning of short and long fibers in the sheet, three-dimensional fiber alignment, and preforming of one or more fiber layers.

The expertise gained during the project could also be used to develop other processes using high-power ultrasounds: clarification; deinking; solid waste agglomeration; turbulence; flocculation; enhanced combustion in recovery boilers.

A very stimulating review of industrial applications of sound was recently published in the January 95 issue of Delta Sky Magazine.¹

PROJECT HISTORY

Project F008 was initiated in July 1992. Design, construction, and preliminary testing of a small-scale acoustic cell to study acoustic radiation pressure effects on water suspended fibers were completed during FY 92-93. The construction of a basic experimental setup was undertaken during FY 93-94. Qualitative observations of fiber agglomeration at various flow rates and consistency levels (up to 1%) were obtained during the second year.

ACCOMPLISHMENTS

The following activities were accomplished:

- Acoustic Cell Characterization (Mr. Troy Runge, M.S. Student; Mr. Joe Gehardstein, Assistant Engineer)

The relationship between the electrical power delivered to the transducer and the useful power in the acoustic cell was determined. Also, two independent methods were successfully tested to evaluate the acoustic force acting on cylindrical particles. Results were used to validate the procedure to measure the acoustic power.

- Acoustic Wet Fiber Flexibility (Mr. Troy Runge, M.S. Student)

A series of experiments were performed to demonstrate the concept of wet fiber flexibility using single-fibers mounted as cantilever beams. Observations indicated that the fibers did not generally deflect as expected even though the acoustic power was more than adequate. Instead, fibers were broken (refined) by the distributed acoustic load. This phenomenon was attributed to

the viscoelastic properties of wood pulp fibers. In the presence of a high frequency oscillating load, fibers cannot relax. As a consequence, there is a buildup of stiffness and an apparent increase of brittleness.

- Acoustic Wet Fiber Compressibility (Mr. Troy Runge, M.S. Student)

Unexpected results about fiber flexibility led to the rapid development of a modified setup to study the compactibility of a fiber mat in the acoustic cell. An optimized traveling wave field was used. Results obtained using Kraft softwood fibers subjected to five different beating levels provided enough evidence to support a simple relationship between acoustic compactibility and beating level.

- Acoustic Fiber Separation/Fractionation (Mr. Keit Ma, M.S. Student; Mr. Joe Gehardstein, Assistant Engineer)

A mechanical divider with two output streams was installed on one end of the acoustic cell to demonstrate the concept of acoustic fiber separation/fractionation. A traveling wave field separation configuration was implemented. The system is operated in a batch mode. Preliminary observations showed that high and low consistency fractions are easily obtained.

- Acoustic Fiber Agglomeration and Reorientation (Mr. Joe Gehardstein, Assistant Engineer)

The development of a laser-based optical system to monitor the motion of fibers in the acoustic field was completed. Various polarization schemes are now investigated to detect fiber reorientation independently from fiber agglomeration.

- Ultrasonic Deinking (Mr. Eric Watkins, Ph.D. Student - A390 Problem)

An exploratory study of a novel ultrasonic concept to separate ink particles from fibers was conducted.

- Research Proposal Titled: "Acoustic Fiber Fractionation"

In response to a Notice of Program Interest from the Department of Energy, a proposal was completed in October 1993 to demonstrate the concept of acoustic fiber fractionation from laboratory- to pilot-scale level. Results from the competition are not available yet.

EXPERIMENTAL SETUP

A schematic of the basic experimental setup to study water-suspended fibers interacting with an acoustic wave field is depicted in Figure 1. One distinguishes on the right side an in-line acoustic cell mounted vertically to decouple gravitational and acoustic fields. A peristaltic pump is used to precisely control the flow rate in the continuous flow loop. Zero-flow and laminar flow conditions are possible. The suspending medium can be either tap or degassed water. A constant temperature circulator is available to perform experiments at different temperature levels. Fiber consistency can be up to 1%.

A schematic of the acoustic cell is shown in Figure 2. It consists of four identical and removable modular wall sections. These sections are used to support either a transducer, a reflector plate, an absorber plate, or a viewing port (glass window). The nominal length and width of these components are 100 mm and 20 mm, respectively. Figure 2 illustrates the case of a one-dimensional unbalanced resonator configuration (transducer-reflector assembly).

The narrow-band, single-element transducer was designed to resonate at 150 kHz. Its rectangular cross section ensures that every fiber penetrating the acoustic field is submitted to the same acoustic dwell length. Considering an approximate sound velocity in water of 1500 m/s at room temperature, the acoustic wavelength is 10 mm. When a standing wave field is prescribed (transducer-reflector assembly), four agglomeration planes are produced. When a traveling wave field is used (transducer-absorber assembly), fibers are pushed against the absorber.

A computer-controlled function generator and a broadband power amplifier are used to drive the transducer. A rod-mounted, calibrated, 5 mm diameter, sub-MHz P(VDF-TrFE) hydrophone is used to evaluate field uniformity, pressure, and power in the acoustic cell. Acoustic wavelength and power are stabilized against temperature variations by using a thermocouple mounted on the transducer and a computer-controlled temperature compensation system. A CCD camera and an imaging system are used to record ARP effects. An argon-ion, laser-based system is also used to study agglomeration and reorientation effects. The optical system is further described below.

ACOUSTIC CELL CHARACTERIZATION

We invested a fair amount of time during the past year to establish a relationship between the electrical power delivered to the transducer and the acoustic power. We were also able to develop two independent methods to determine the acoustic radiation force acting on the fibers (standing wave field configuration). Since there was good agreement between the two methods, we were able to validate the accuracy of acoustic power measurements.

The calibrated hydrophone was used to determine the acoustic power. It was mounted to a three-dimensional translation system located above the acoustic cell. An oscilloscope was used to determine the AC signal at 150 kHz. Figure 3 shows a mapping of the RMS acoustic power as obtained every 0.5 mm from the transducer's position to the reflector's position. The RMS electrical power was set to 51.4 W. It was not possible to get data near the reflector due to physical constraints. The dashed line represents the predicted acoustic power for an ideal resonator; it is calibrated to fit experimental data. Results show that the resonator is far from ideal (perfect plane standing wave field everywhere in the cavity). Contrary to expectation, the acoustic power is not constant from node to node. Possible explanations are transducer's edge effects due to the relatively small dimensions of the acoustic cell, sound scattering in the cavity, inhomogeneity of the transducer's surface.

It is interesting to note that the maximum measured acoustic power is approximately $50 W_{\text{RMS}}$ for a 51.4 W_{RMS} electrical power. This would tend to support that the electrical and mechanical coupling efficiencies in the system are near ideal conditions. But this is not the case as we know that the impedance matching conditions between the power amplifier and the transducer are not optimized. Instead, the reason is that there is a buildup of power due to resonance.

Two independent methods were tested to evaluate the acoustic force acting on water-suspended cylindrical particles. In the first method, we used the hydrophone to determine the acoustic pressure (proportional to acoustic power) and the theoretical equation² to predict the acoustic force acting on a rigid cylinder in a standing wave field. This equation is a function of the acoustic pressure, p_0 .

$$F_{sw} = f(\beta) \frac{\pi a^2}{2} \bar{E} k \sin[2 k h] \quad (1)$$

where $f(\beta) = \left[\frac{2(1-\beta)}{(1+\beta)} + 1 \right]$ is the inertia factor; $\beta = \frac{\rho_0}{\rho_1}$ is the ratio of the suspending medium

density to cylinder density; $k = \frac{2\pi}{\lambda}$ where λ is the acoustic wavelength; $\bar{E} = \frac{1}{2\rho_0} \left(\frac{p_0}{c} \right)^2$ is the

mean energy density; p_0 is the static pressure (RMS acoustic pressure); c is the sound velocity; h is the cylinder center of mass position with respect to a nodal velocity plane.

The second method was developed during the course of single-fiber wet flexibility experiments (see below). The procedure for fiber flexibility involves mounting fibers on the tip of a metal rod which can be positioned anywhere inside the acoustic cell. We found that the metal rod deflected upon the onset of the acoustic field. Taking advantage of this effect, we were able to use the imaging system to gather quantitative measurements of the distributed acoustic load. This was accomplished by comparing images obtained without and with the acoustic field. A schematic of the deflection arrangement is shown in Figure 4. The distance b corresponds to the section of the rod located within the acoustic cell.

For the case of a cantilever beam subjected to a distributed force, the tabulated equation relating the force and maximum deflection is as follows:

$$F = \frac{24EI\delta_B}{(3L^4 - 4a^3L + a^4)} \quad (2)$$

where δ_B is the maximum deflection.

Figure 5 shows a typical image analysis result. Also shown in this figure are rod parameters and the measured acoustic force. The modulus of elasticity was found from experiments using the rod as a cantilever beam. The rod was mounted horizontally, and a small weight was attached to its free end. The measured value, i.e., 194 GPa, agrees with tabulated data for mild steel.

Force measurements using the hydrophone method (electrical) and the rod deflection method (mechanical) are shown in Figure 6 as a function of the electrical power. Measurements were obtained at constant rod position with respect to the transducer. Since the two methods are based on very different measuring principles, the agreement is well above expectations. If one plots rod deflection force measurements as a function of hydrophone force measurements for various rod positions and power levels, a linear relationship is obtained. This is shown in Figure 7. Since the correlation is very good ($R^2 = 0.94$), we can validate the hydrophone method to determine the acoustic power. Moreover, we have an experimental confirmation of Equation 1. The 17% offset between mechanical and electrical measurements can be attributed to several factors: pressure measurements are affected by the physical size of the hydrophone; hydrophone and rod have different geometries, hydrophone calibration may be off.

ACOUSTIC WET FIBER FLEXIBILITY

One of the objectives of Project F008 concerns the demonstration of a noncontact acoustic method to determine the flexibility of wet fibers. It was first decided to investigate the flexibility of cantilever-mounted single fibers subjected to a distributed acoustic load in a standing wave field. A schematic of the testing method is shown in Figure 8.

Maximum deflection at point B is given by

$$\delta_B = \frac{F_{sw} \ell^4}{8EI} \quad (3)$$

Thus, assuming that F_{sw} can be determined using Equation 1 and the hydrophone, and that δ_B can be evaluated using image analysis, the flexural rigidity EI can be obtained. Assuming the following parameters:

- RMS Acoustic pressure, p_0 : 200 kPa
- Sound velocity in water at room temperature, c : 1480 m/s
- Density of water, ρ_0 : 1000 kg/m³
- Fiber radius, a : 25 μ m
- Acoustic wavelength, λ : 10 mm

the predicted acoustic force per unit length, F_{sw} , at $h = \lambda/8$ is 5.6×10^{-6} N/m (see Eq. 1). Using Tam Doo and Kerekes³ flexural rigidity results for earlywood and latewood fibers (Kraft pulp, unbeaten), one can predict the following deflections for 2 mm fibers:

- $\delta_{\text{early}} = 1.2 \mu\text{m}$ ($EI = 9.3 \times 10^{-12} \text{ Nm}^2$)
- $\delta_{\text{late}} = 0.4 \mu\text{m}$ ($EI = 26 \times 10^{-12} \text{ Nm}^2$)

A three-dimensional translation system located above the acoustic cell was used to position a steel rod anywhere in the acoustic field. Never-dried fibers were attached to the rod using a clamping device. Fibers were imaged using the CCD camera.

Observations using Loblolly Pine fibers indicated that contrary to expectation, fibers did not generally deflect when the acoustic field was turned on, even though the acoustic power did not seem to be a limiting factor. Figure 9 illustrates typical observations. We found that some fibers could not sustain the intensity of the acoustic load; they experienced damage within a few seconds of exposure (see top-right and bottom-left images). Although not fully explored, we made the assumption that the breaking points were associated to defects in the fibers. It was also observed that just before separation, fiber tips, now presumably subjected to acoustic streaming, were capable of inducing mechanical deflection of remaining fiber sections (see top-right image). Also, we observed some fibers with induced vibrations (see bottom-right image).

The following interpretation is proposed to explain the behavior of cantilever-mounted fibers in the acoustic field. Considering that wood pulp fibers have viscoelastic properties, lack of relaxation time during each oscillation (150,000/sec) of the acoustic field will induce an apparent increase of stiffness, which will lead to an apparent increase in fiber brittleness. Thus, instead of bending, fibers will break. One should note that the increase in fiber brittleness is not permanent and will disappear upon removal of the acoustic field. Also, fiber stiffness under no-cyclic conditions is unaffected. Thus, bending under mechanical loading conditions can still occur (as seen in Figure 9 - top-right image).

We have here a possible basis for the concept of acoustic refining. It has long been thought that an acoustic field could deliver enough power to cut fibers and induce fibrillation.

It is of interest to establish a parallel with the use of an acoustic field to reduce the size of laser ink particles (ultrasonic deinking).

ACOUSTIC COMPACTIBILITY OF A FIBER MAT

Considering that the concept of acoustic wet fiber flexibility did not work as expected (although we obtained evidence of refining), it was decided to abandon single-fiber testing and move ahead with the investigation of another concept related to flexibility. It was long thought that one might be able to get some very useful information about the compactibility of a fiber mat using a traveling wave field.

The concept is illustrated in Figure 10. A fiber suspension is first transferred to the acoustic cell using the flow system (see Figure 1). Then, assuming that the suspension is at rest (zero flow) in the acoustic cell, the field is turned on. Depending upon fiber flexibility and the intensity of the acoustic power, the suspension will slowly or rapidly compact against the absorber. One can denote the cross-sectional area of the fiber mat by A . While it is hypothesized that this area is related to the degree of compactibility of the fiber mat (at constant acoustic power), it is also sensitive to consistency. In order to eliminate the consistency dependency, we can go a step further and turn the field off. The fiber mat will then spring back. Denoting the new cross-sectional area by A' , one can relate the degree of compactibility to the differential cross-sectional area ΔA or compaction area, i.e., $A' - A$.

The concept was demonstrated using bleached Kraft softwood fibers beaten to several freenesses using a Valley beater. A schematic of the experimental setup is shown in Figure 11. The imaging system was used to record areas A' and A , and compute ΔA . Figures 12, 13, and 14 show selected photographs of compacted fiber mats (acoustic power on, A ; acoustic power off; A' , Xor operation, ΔA). For comparison, the acoustic power is constant ($30 W_{RMS}$). The nonuniformity of the fiber mats is directly related to the transducer's nonuniformity (this problem can be solved by the availability of a more uniform transducer). When compared to the suspension consistency, the fiber mat consistency is about 1.5 to 2 times higher (it could be more with more power). A closer look at Figures 12 and 13 indicates that the fiber compaction is higher as the beating time is increased (higher ΔA).

The compaction area as a function of beating time is plotted in Figures 15 and 16 for two different power levels. Each plot includes results obtained for two different consistencies (0.5 and 1%). While results do not appear to depend on consistency, one can clearly see that the compaction area increased as the beating time is increased. One might expect to gather more conclusive results having a better quality transducer and more power. Also, additional experiments are required to further understand the relationship between compactibility (flexibility) and refining, and to optimize the system.

The concept of acoustic compactibility is of particular interest because it could readily be implemented for on-line monitoring of refining. Dilution and degassing would not be required.

ACOUSTIC FIBER SEPARATION/FRACTIONATION

Consider a rigid cylindrical particle of radius a free to move in a traveling wave field in which the wave normal is perpendicular to the axis of the cylinder. A derivation of the acoustic force acting on the cylinder was obtained by Awatani:⁴

$$W = \frac{SE}{2(ka)^2} \left[2(w_{0r}R_2 + w_{0s}I_2) + \sum_{m=0}^{\infty} \{m(m+1) - e_m(ka)^2\} \{R_m R_{m+1} + I_m I_{m+1}\} \right] \quad (4)$$

where

$S = \pi a$: Projective area of the cylinder;

$E = \rho_0 k^2 A^2 / 2$: Energy density of the field;

k : Wave number;

A : Amplitude of the acoustic field;

ρ_0 : Density of the suspending medium.

Other parameters in this equation are tedious functions of Bessel and Hankel's functions. In his paper, Awatani supplied a plot of W/SE vs. ka for various cylinder densities. Assuming that k is constant, it was shown that the acoustic force increases as the radius increases. This is also the case for the acoustic force acting on a rigid cylinder in a standing wave field (See Equation 1).²

The dependency of the acoustic force upon the cylinder radius is the basis for the separation technique. Accordingly, the larger is the cylinder radius, the larger is the acoustic force, and hence, the larger is the migration process in the acoustic field. Thus, one should expect coarser wood pulp fibers to agglomerate at a faster rate than slender fibers and/or fines. One should mention that the

dependency of the acoustic force upon the cylinder wall thickness is not considered in Awatani's treatment.

In order to demonstrate the concept, the experimental setup was modified to operate in a batch mode. A schematic of the separation system is shown in Figure 17. The top transparent viewing section in Figure 1 was replaced by a section containing an adjustable mechanical divider with two output streams. An absorber was installed in the acoustic cell to optimize the propagation of a traveling wave field (see above Section on compactibility). The system is not pressurized.

The maximum available flow rate was found to be approximately 1450 ml/min. The maximum acoustic power was limited to 30 W_{RMS} to extend the life of the transducer (Note: after two years of intensive use, the prototype transducer clearly shows signs of rapid deterioration and is no longer as effective as it used to be).

After several unsuccessful trials (the mechanical divider was modified three times), we were able to get the system working in a satisfactory manner. Some problems, which are somewhat related to the small-scale of the system, still exist. For instance, if the acoustic power is too high for a certain flow rate, agglomerating fibers are held against the absorber by the acoustic force and do not exit the acoustic cell. Eventually, large chunks of fibers will accumulate and will be removed by the flow. This "sticking" problem is attributed to the rubbery surface of the absorber. It can be partially alleviated by spraying a thin film of Teflon on the absorber's surface.

Figures 18 and 19 show photographs of rayon fibers circulating in the acoustic cell and the divider section when the acoustic field is off and on. Fiber length and denier are 3.2 mm and 3, respectively. The consistency is 0.25%, and the flow rate is 1000 ml/min. One can easily see in Figure 19 the

agglomeration process in the acoustic cell as fibers are moving upward. Output streams have different consistencies.

Other qualitative observations were obtained using softwood and hardwood fibers at consistencies up to 0.5%. Video recordings are available.

Experiments are now underway using a matrix of rayon fibers (different deniers and lengths) to optimize the system. Effects of flow rate and acoustic power are studied. The separation efficiency is also determined. Another series of experiments is scheduled to begin soon using classified wood pulp fibers. Satisfactory progress may be hindered by the poor performance of the transducer.

ACOUSTIC FIBER AGGLOMERATION AND REORIENTATION

A. Optical Monitoring Systems

Information concerning the amount of agglomeration, speed of agglomeration, as well as rotation of wood pulp fibers due to the acoustic field is determined with a continuous wave laser and polarized light. Figure 20 shows one of the optical system setups that is currently being used.

Polarized light is supplied by a single-mode, half-watt, Ar:Ion laser operating at the 514.5 nm line. The light is expanded using a beam expander to give roughly a 1 inch diameter beam. The beam then travels through a neutral density filter used to control the laser intensity at the photodetector. As agglomeration is expected to occur at specific areas in the test cell, a filter grating is inserted into the beam path just before the test cell. This filter grating allows light to enter the cell only at places in which agglomeration will occur. When the polarized light enters the test cell, it is scattered by fibers in the cell and exits with a random polarization. An

analyzing polarizer oriented perpendicular to the initial polarization axis is used to remove any photons which were not scattered in the test cell. Those photons which pass through the polarizer are collected by the focusing lens and picked up by the photodetector. The output from the photodetector becomes one of the inputs to a differential amplifier. The second input to the amplifier is a variable power supply. The differential amplifier subtracts the two input signals, and provides an output which is viewed on an oscilloscope.

A second optical system that is being used to determine rotation of fibers is similar to the setup in Figure 20, except a quarter wave plate is inserted between the neutral density filter and the filter grating. The quarter wave plate rotates the laser's polarization to make it circular. Hence, when the laser enters the test cell, the light is circularly polarized. As the light passes through the test cell, it is scattered by the fibers. The analyzing polarizer is again used, except this time it is rotated through 360 degrees, and measurements of the amount of light entering the photodetector are made during the rotation.

B. Current Experiments

Two types of experiments are currently being done using the laser data acquisition system. The first type of experiment is to determine the speed at which fibers are agglomerating. The second type of experiment is to measure the amount of and speed of rotation the fibers undergo during agglomeration. As of now, we are still acquiring the final pieces of equipment and fine tuning the optical system. Some encouraging data have been taken using these two techniques, but until the systems are fully up and running, we cannot be sure of our results.

B.1 Speed of Fiber Agglomeration

In this experiment, the system shown in Figure 20 is used. Fiber concentrations around 0.001% are used so as to prevent multiple scattering of single photons in the test cell. A continuous flow of fibers through the cell is made possible by an external flow loop. At the start of an experiment, the acoustic field is off, and fibers flow through the cell at a low flow rate. At time = 0, the acoustic field is switched on, and the output of the differential amplifier is recorded using an HP voltmeter. As agglomeration begins to occur, an increasing amount of light is scattered by the fibers. This scattered light is picked up by the photodetector and is recorded by the voltmeter. After approximately two seconds, the acoustic field is switched off, and the experiment ends. Plots of scattered light versus time are made showing the rate at which agglomeration occurs. We will be using rayon fibers of various deniers and lengths to characterize the acoustic radiation pressure and determine its effectiveness in moving fibers.

B.2 Rotation of Fibers During Agglomeration

In this experiment, the second setup described in Section A is used. Again, fiber concentrations around 0.001% are used to prevent multiple scattering of single photons in the test cell. Continuous flow of fibers at a low flow rate is also again provided by an external flow loop. At the start of the experiment, the acoustic field is on, and fibers are agglomerating into planes. Circularly polarized laser light enters the test cell and is scattered by the fibers. An analyzing polarizer on the exit side of the test cell is rotated through 360 degrees, blocking certain polarizations of light as it is rotated. Polarizations which are not blocked are allowed to pass through the polarizer and are absorbed by the photodetector. The output from the differential amplifier is measured on the oscilloscope, and plots of transmitted light versus polarizer angle are made. In this experiment, we hope to show that as the fibers are rotated in the acoustic field,

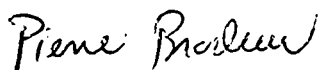
the polarization of the light exiting the cell also rotates. We can then use the rotation of the polarization to monitor fiber rotation.

Measurements of rotation versus time are also possible with the second setup of Section A. In this case, the analyzing polarizer is set at a specific angle, and the output of the differential amplifier is recorded over time using the HP voltmeter.

We will be using rayon fibers of various deniers and lengths to characterize the acoustic radiation pressure and its ability to rotate fibers.

LITERATURE CITED

1. Frazer, L., Good Vibrations - Extraordinary Advances in Sound-Research Technology, Delta Sky Magazine, 112-119 (January 1995).
2. Brodeur, P., Motion of Fluid Suspended Fibers in a Standing Wave, Ultrasonics 29 301-307 (1991).
3. Tam Doo, P.A. and Kerekes, R. J., A Method to Measure Wet Fiber Flexibility, Tappi J. 64(3) 113-116 (1981).
4. Awatani, J., Study of Acoustic Radiation Pressure (IV) (Radiation Pressure on a Cylinder), Memo. Inst. Sci. Ind. Research Osaka Univ. 12 95-102 (1955).



Pierre H. Brodeur
Assistant Professor of Physics

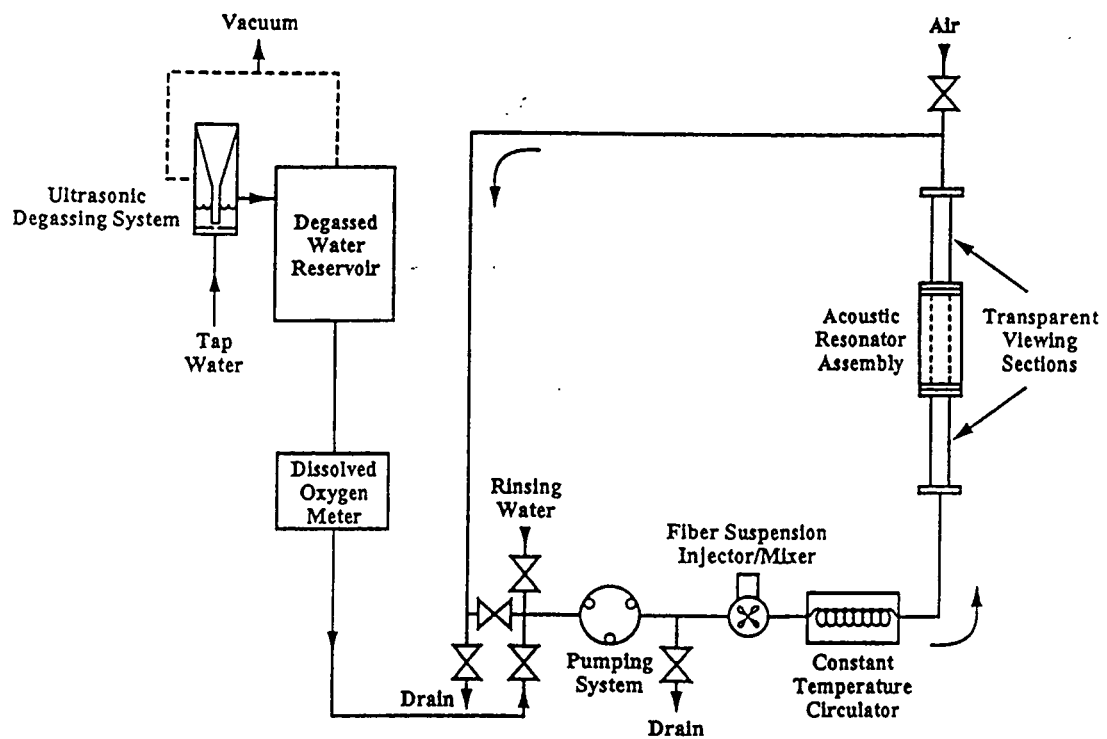


Figure 1. Schematic of the basic experimental setup to study ARP effects.

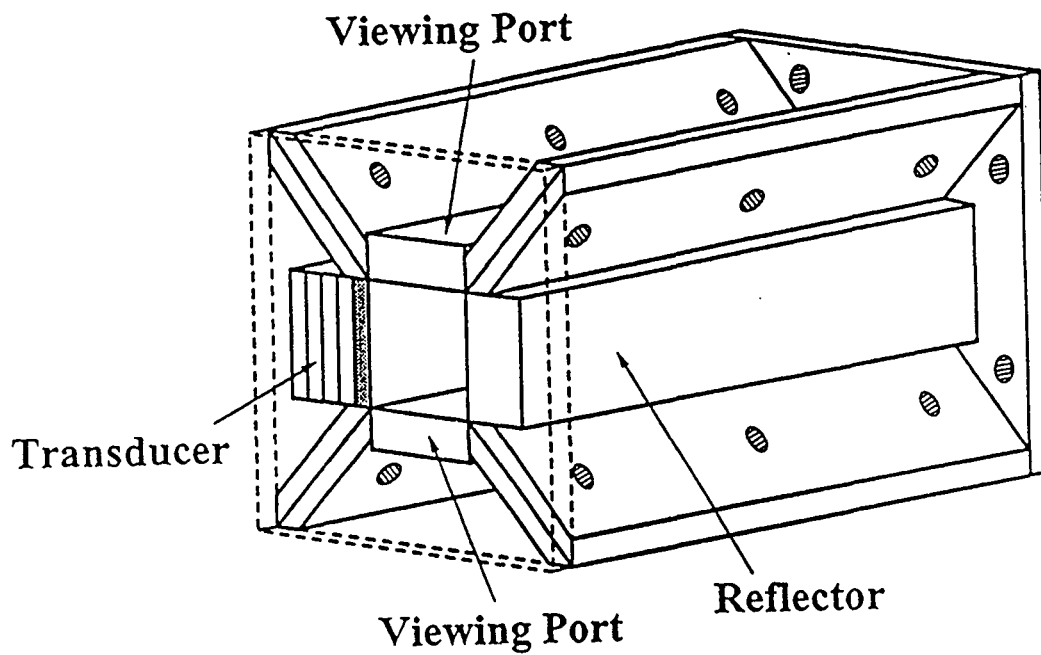


Figure 2. Schematic of the acoustic cell. Components dimensions are as follows: length, 100 mm; width, 20 mm.

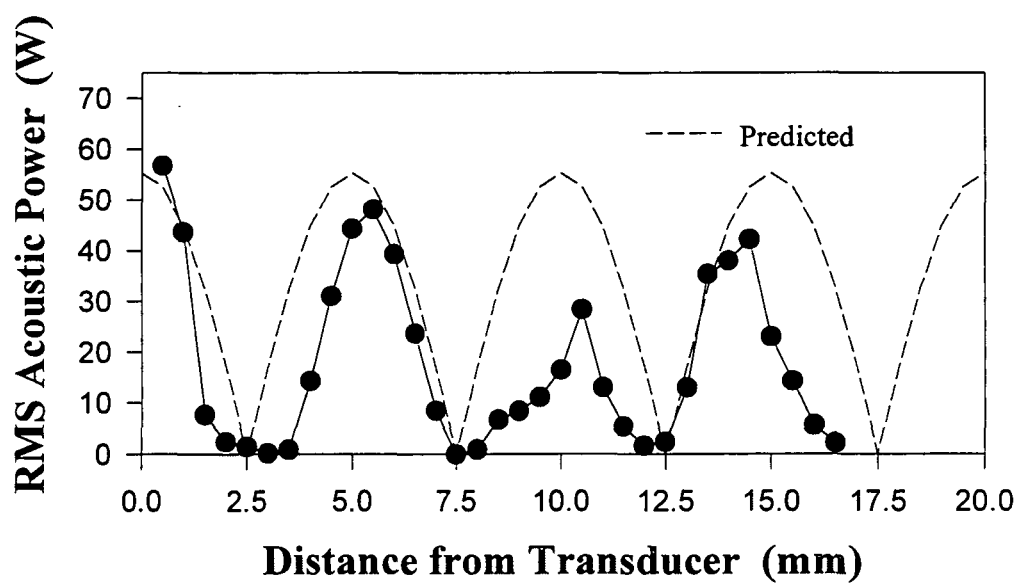


Figure 3. Plot of the RMS acoustic power as a function of distance from the transducer. The dashed line represents the power for an ideal resonator after calibration to fit experimental data.

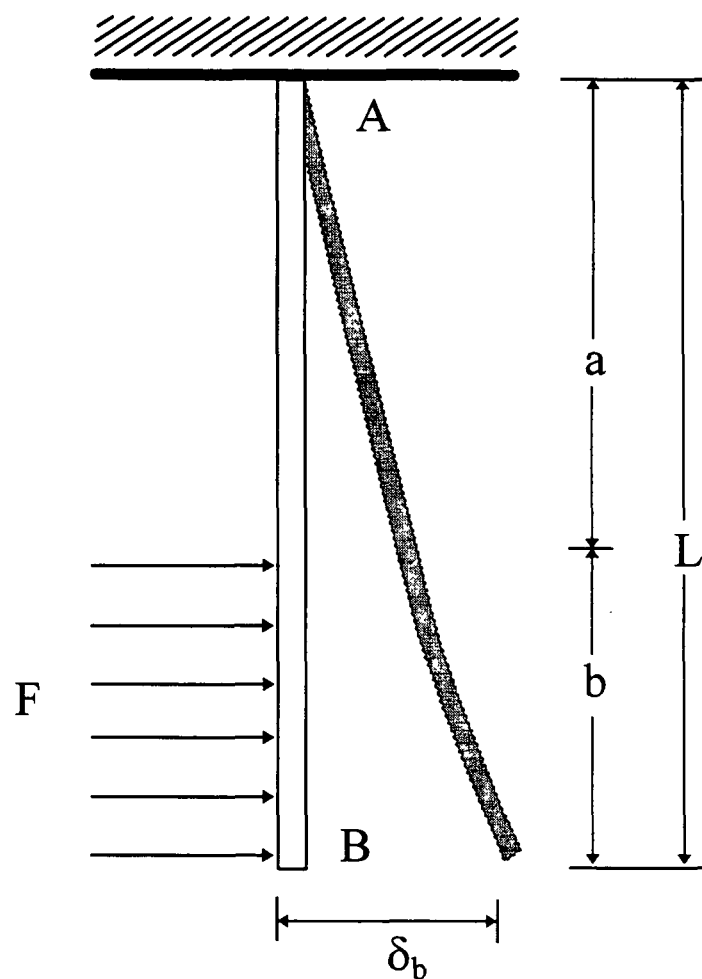


Figure 4. Deflection of a cantilever beam due to a localized distributed acoustic load.



Rod is mild grade steel
 $E = 194 \text{ GPa}$
 $d = 0.50 \text{ mm}$
 $L = 145 \text{ mm}$
 $b = 59 \text{ mm}$
 $\delta_B = 0.0737 \text{ mm}$
 $\text{El. Power} = 33.8 \text{ W}_{\text{RMS}}$
 $\text{Force} = 6.33 \times 10^{-5} \text{ N}$
1 is the initial position
2 is position with
acoustic field on
3 is the deflection (δ_b)

Figure 5. Typical image analysis result of the metal rod subjected to a distributed acoustic load.

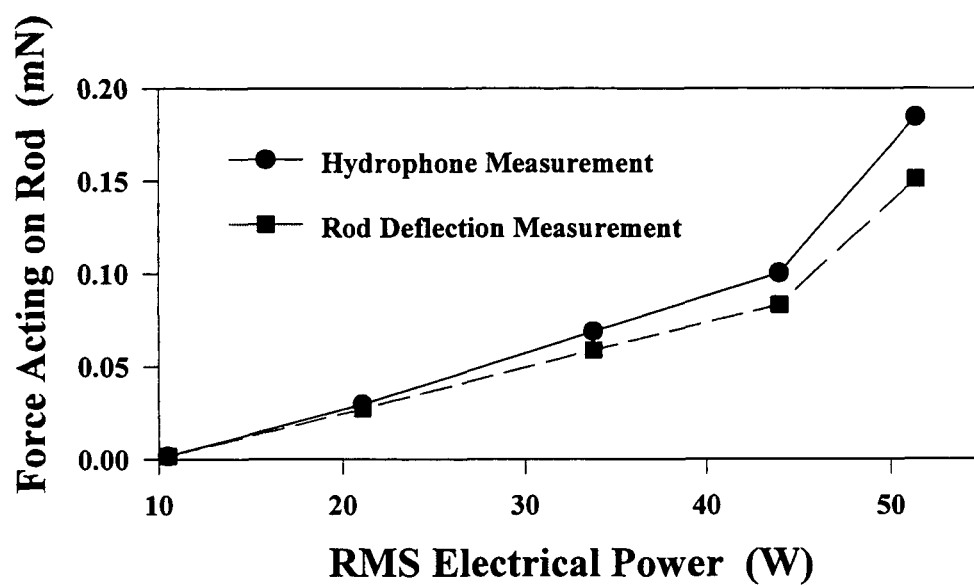


Figure 6. Force acting on the rod as a function of the RMS electrical power. Measurements were obtained at constant rod position with respect to the transducer.

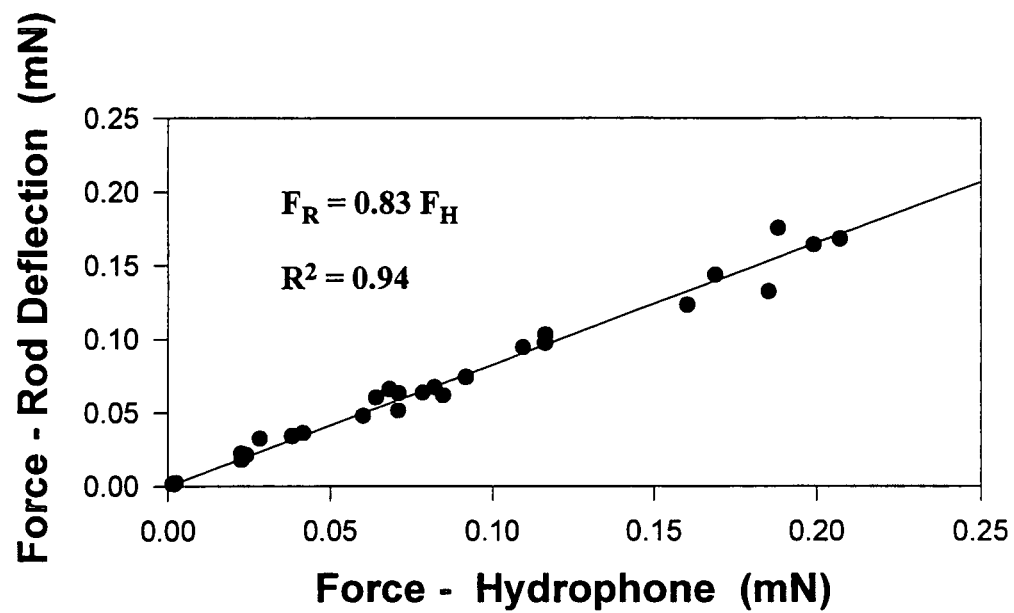


Figure 7. Plot of the force-rod deflection vs. force-hydrophone. Measurements were obtained for various rod positions and power levels.

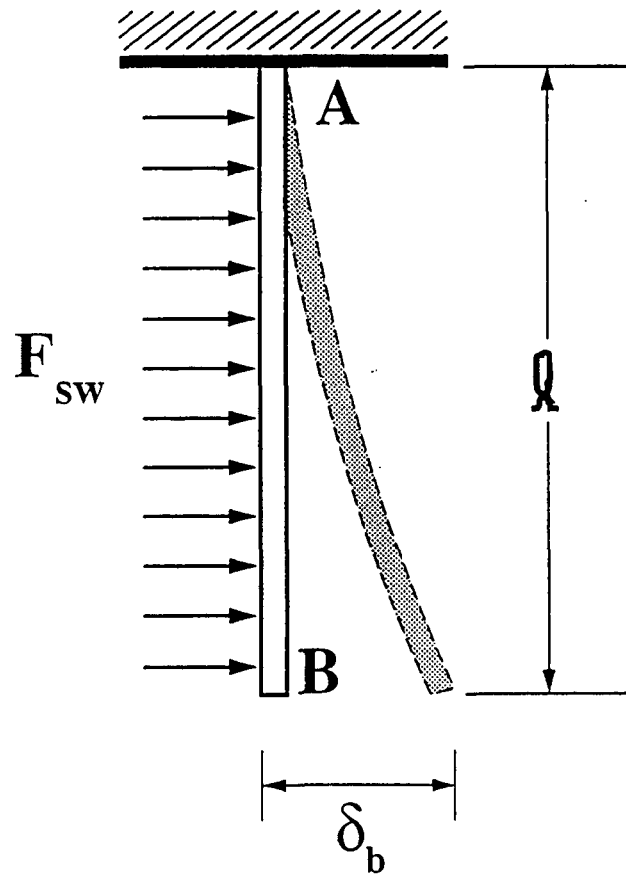


Figure 8. Deflection of a cantilever beam with a uniformly distributed load.

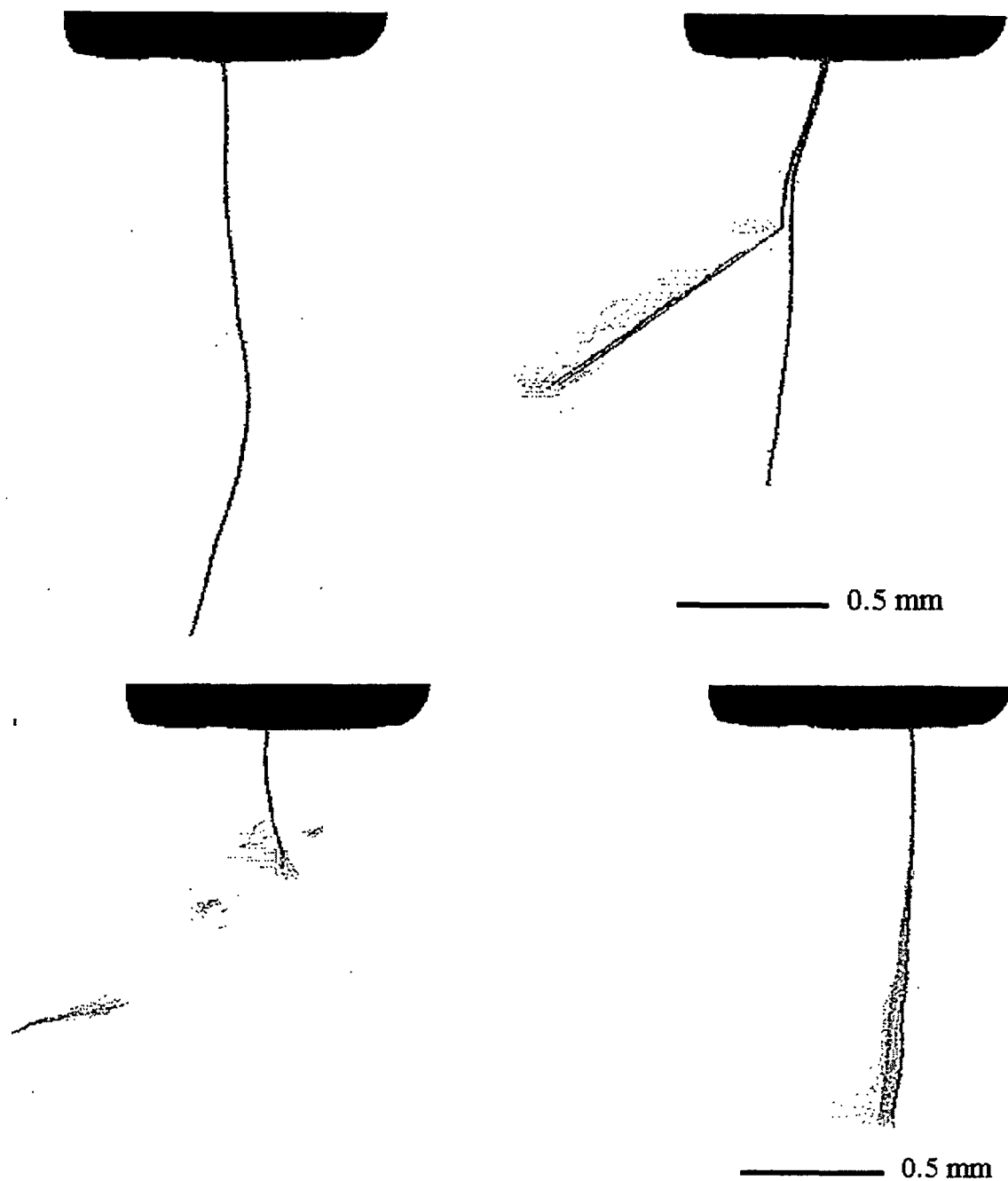


Figure 9. Typical image analysis results of wet fiber flexibility experiments (counterclockwise from top left corner: undeflected fiber when the acoustic field is on; broken fiber; fiber tip removed by acoustic streaming; vibrating fiber).

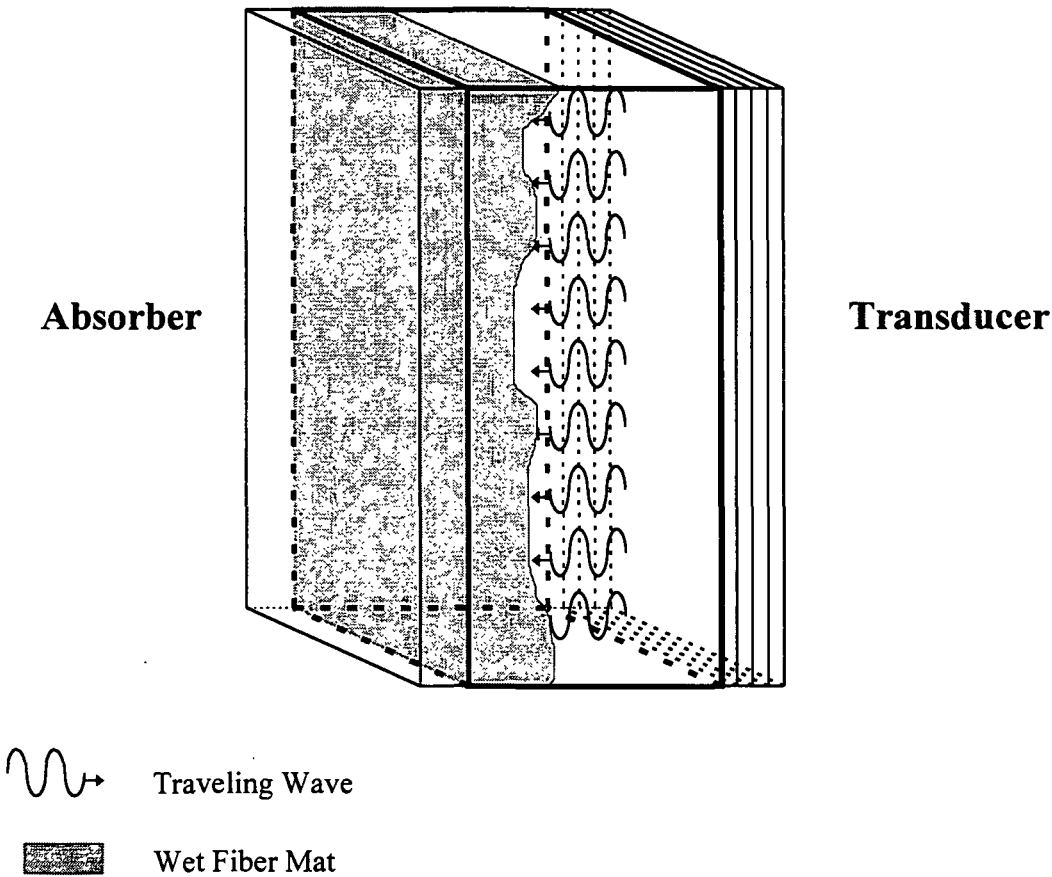


Figure 10. Acoustic compactibility of a wet fiber mat.

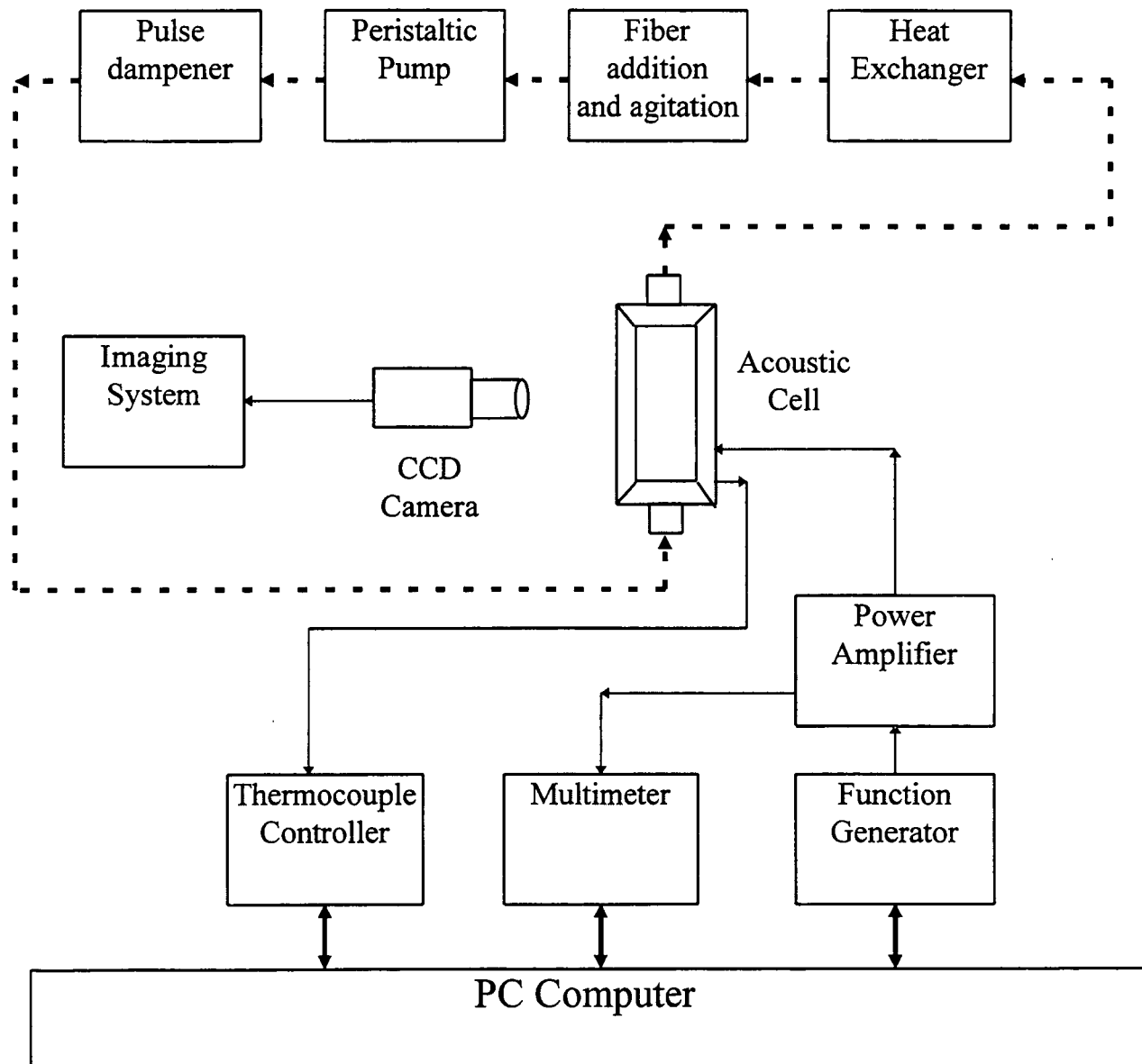
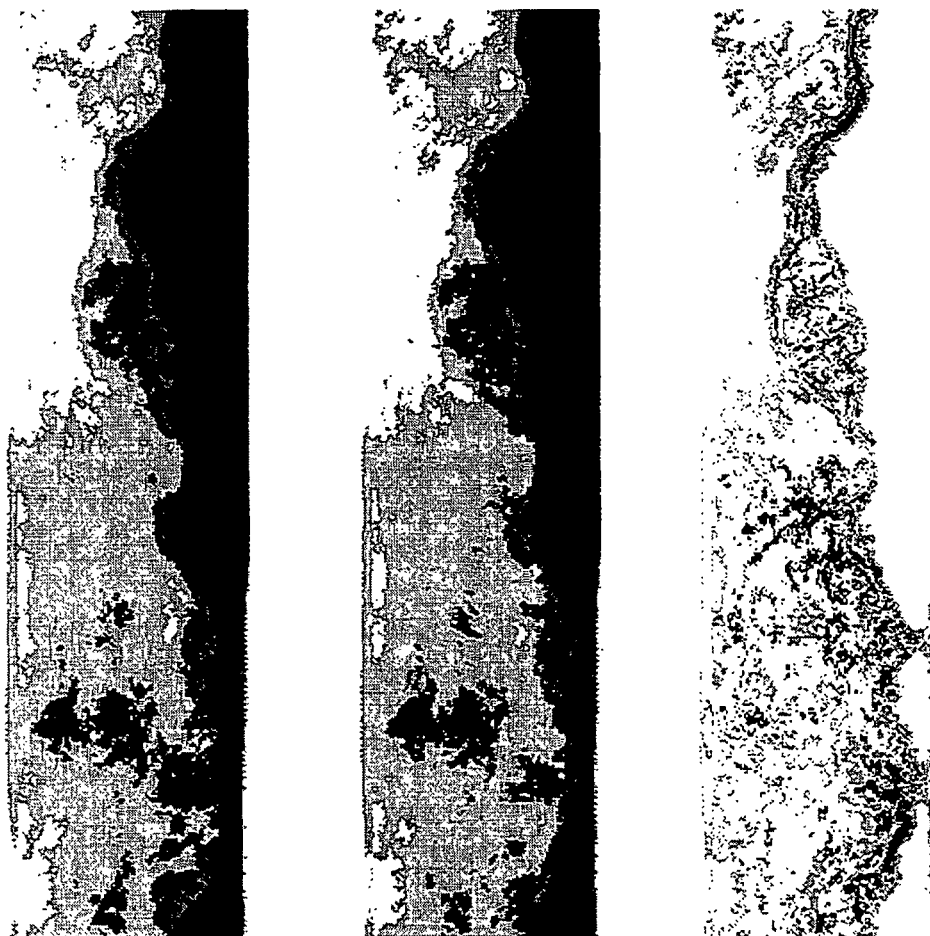


Figure 11. Schematic of the experimental setup for acoustic compactibility experiments.

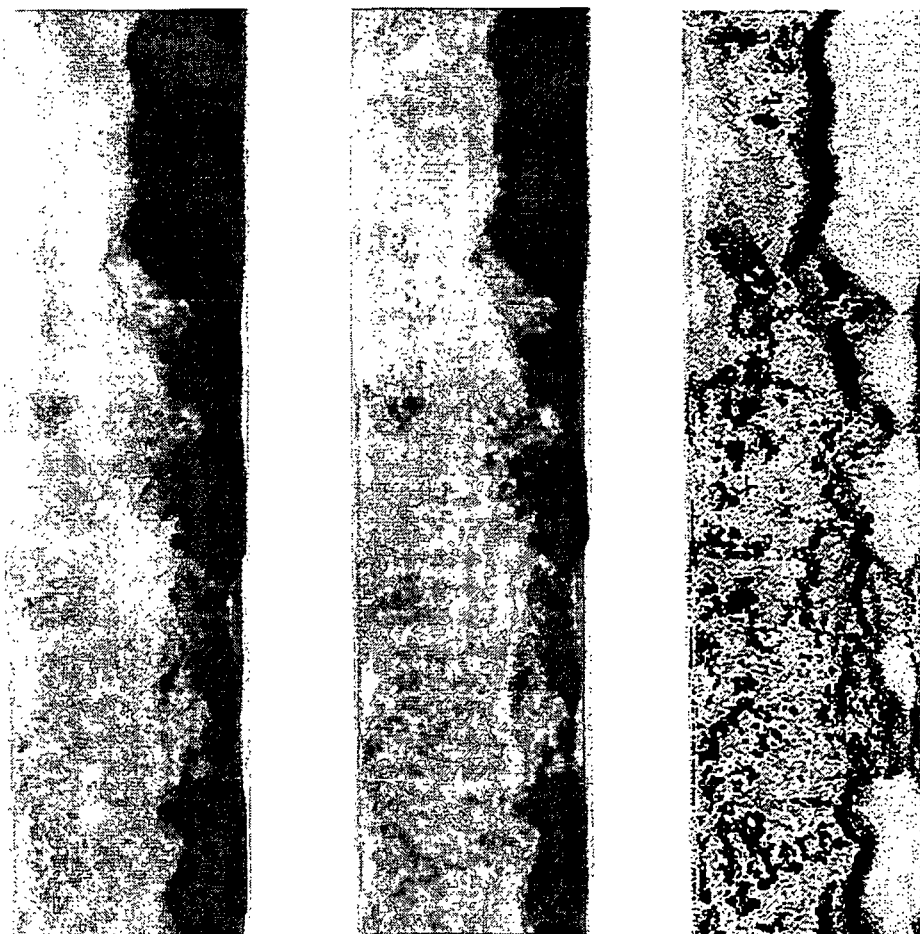


Acoustic
Power on

Acoustic
Power off

Xor
Operation

Figure 12. Images of the fiber suspension in the acoustic cell. Testing conditions are 1% consistency, 5 minutes beating, and 30 W_{RMS} acoustic power.



Acoustic
Power on

Acoustic
Power off

Xor
Operation

Figure 13. Images of the fiber suspension in the acoustic cell. Testing conditions are 1% consistency, 20 minutes beating, and 30 W_{RMS} acoustic power.



Acoustic
Power on



Acoustic
Power off



Xor
Operation

Figure 14. Images of the fiber suspension in the acoustic cell. Testing conditions are 0.5% consistency, 20 minutes beating, and 30 W_{RMS} acoustic power.

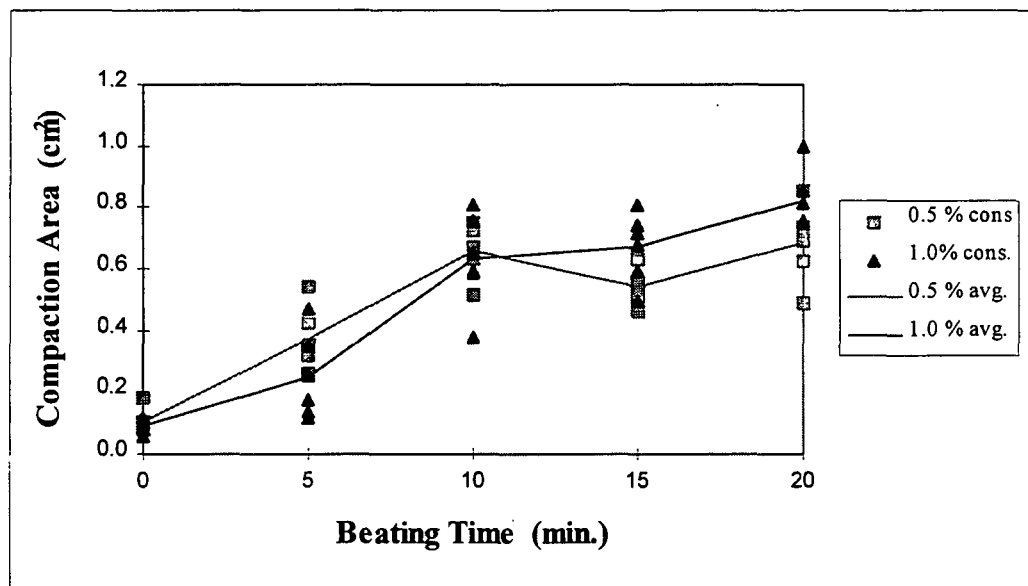


Figure 15. Plot of the compaction area vs. beating time for two different consistency levels. The RMS acoustic power is 20 W.

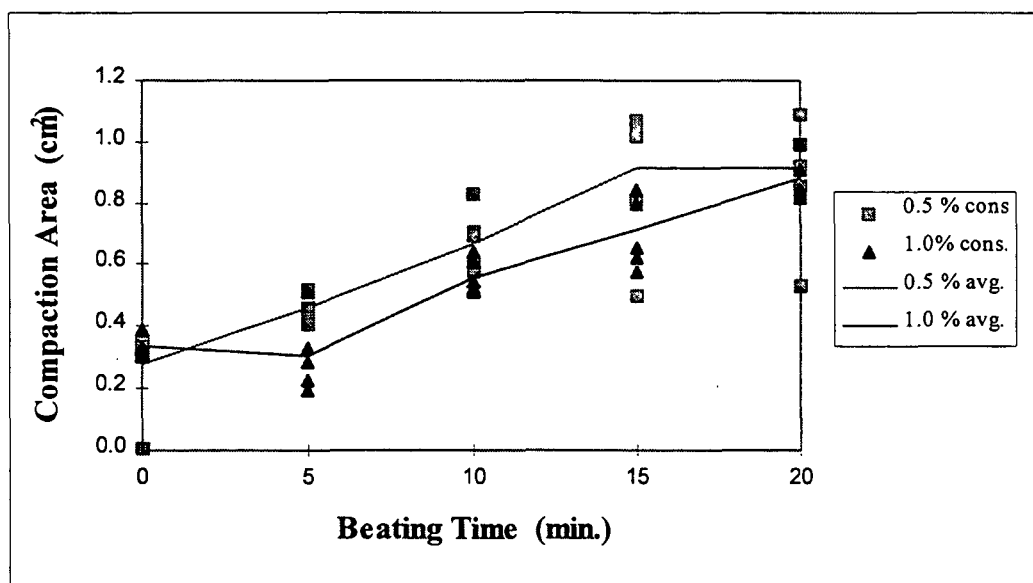


Figure 16. Plot of the compaction area vs. beating time for two different consistency levels. The RMS acoustic power is 30 W.

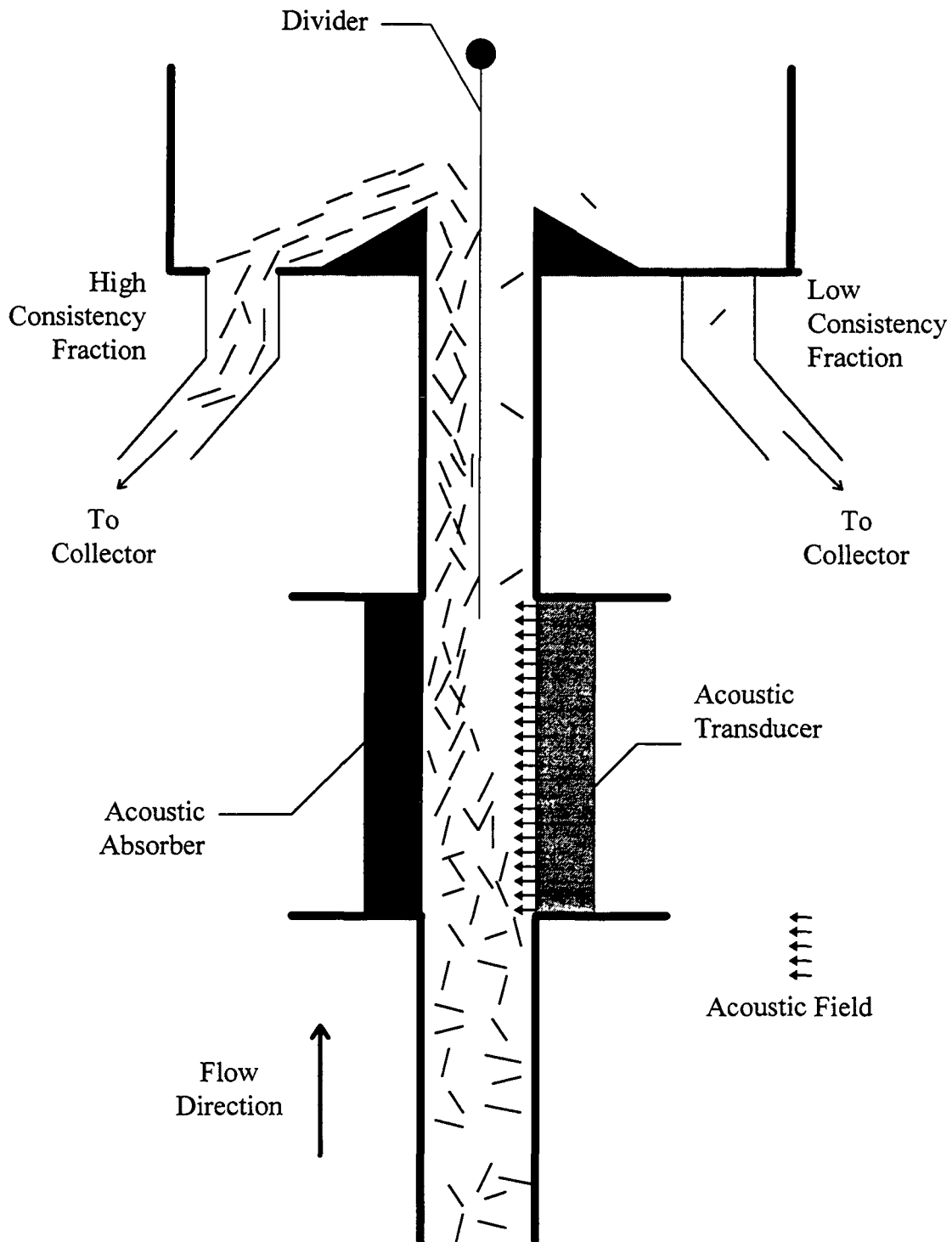


Figure 17. Schematic of the separation system using a traveling wave field.

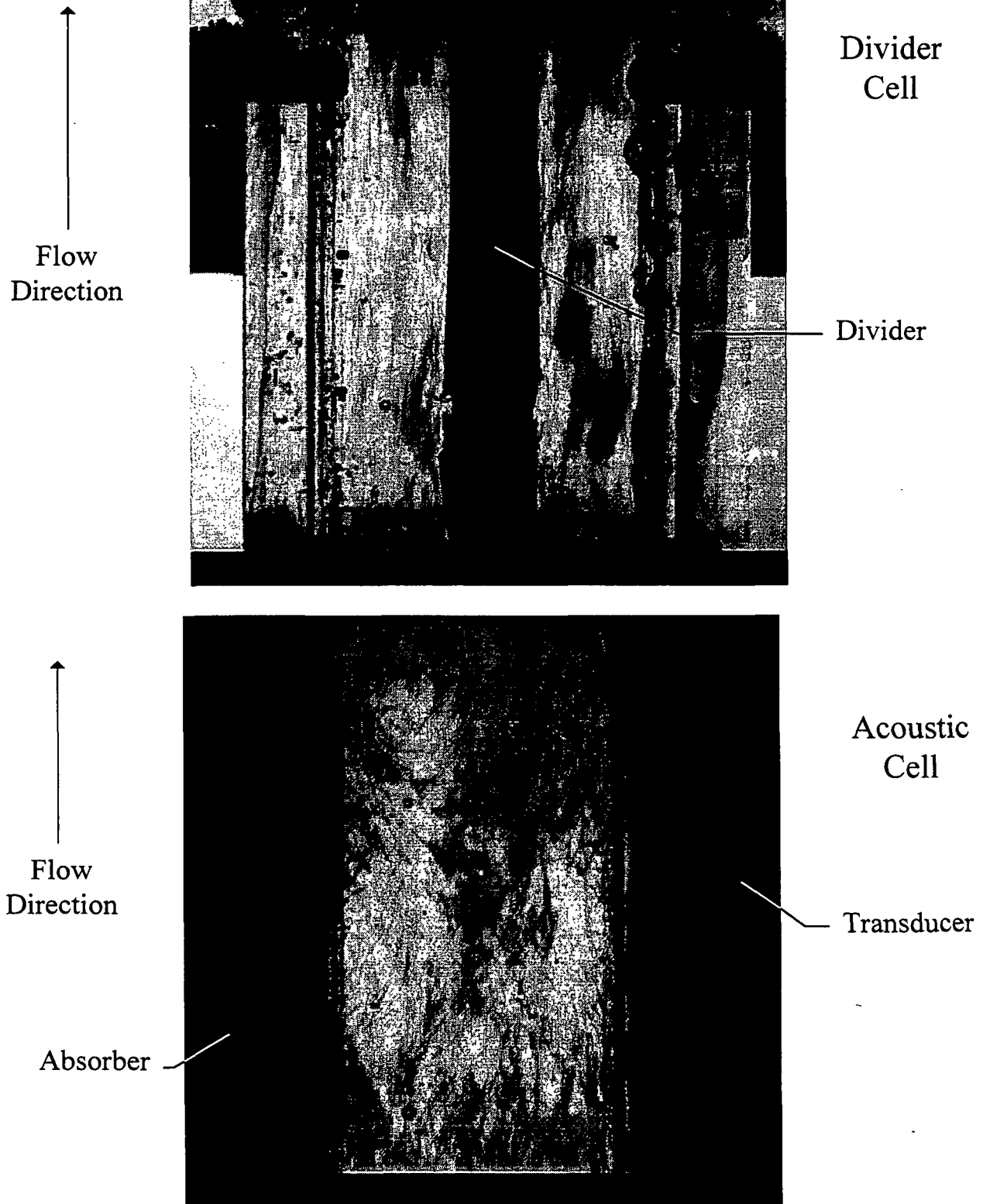


Figure 18. Photographs of acoustic cell and divider section when the acoustic field is off.

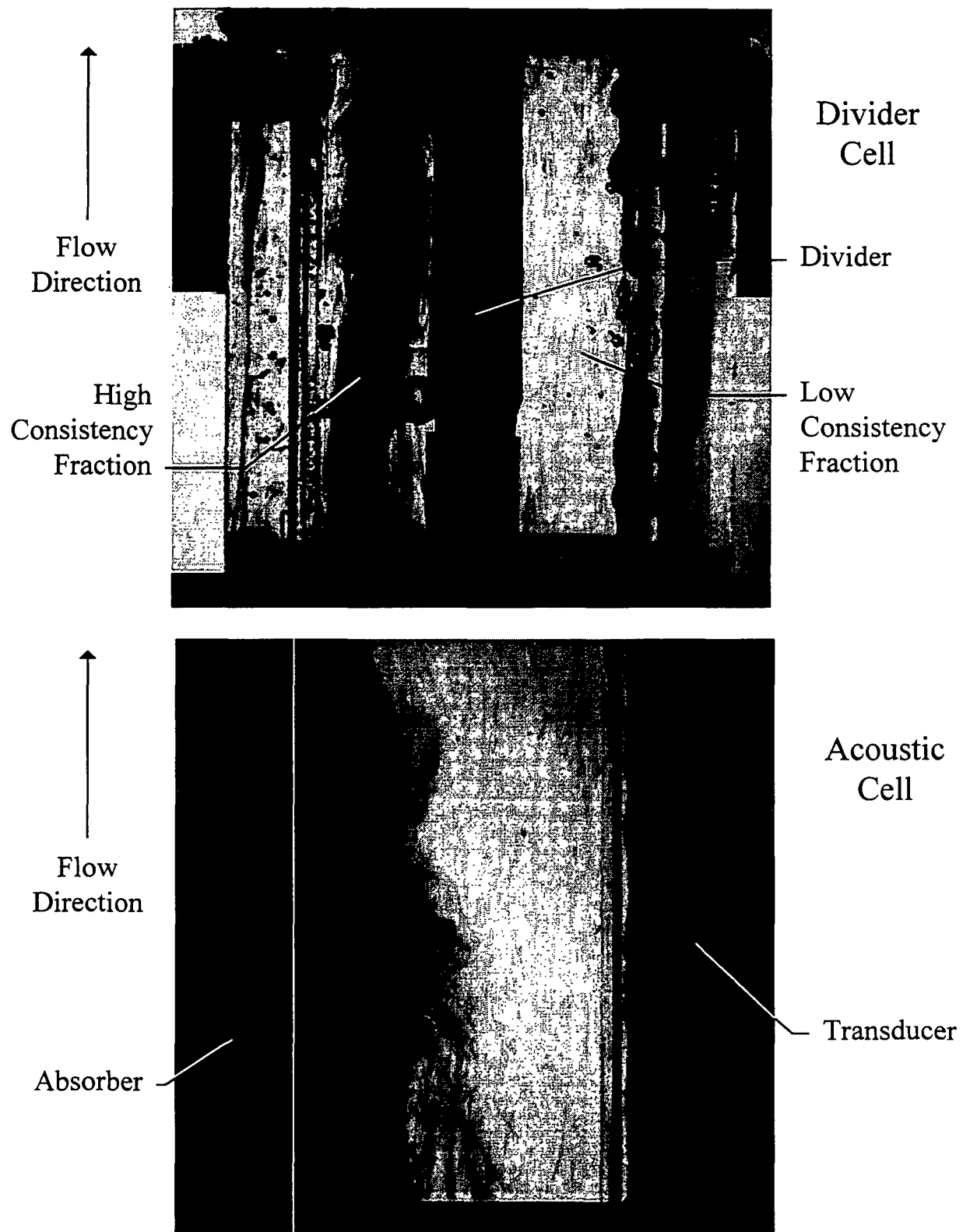


Figure 19. Photographs of acoustic cell and divider section when the acoustic field is on.

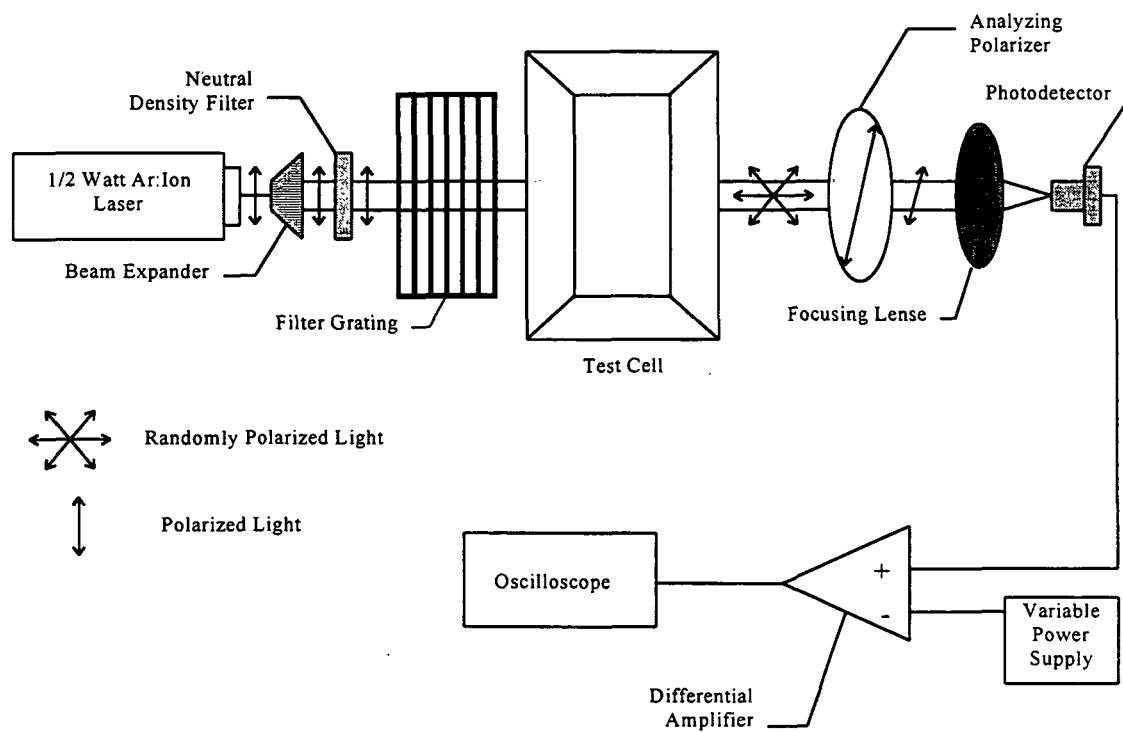


Figure 20. Schematic of one of the optical system setups.